Structure of the cylinder term in the topological expansion

P. Aurenche
Centre de Physique Théorique, Ecole Polytechnique, 91128 Palaiseau Cedex, France (Equipe de Recherche du C.N.R.S. No 174)

L. Gonzalez Mestres*
Laboratoire de Physique Théorique et Hautes Energies Bât. 211, Université Paris Sud, 91450 Orsay, France
(Received 29 August 1977; revised manuscript received 17 January 1978)

We discuss the properties of the cylinder beyond the conventional multiperipheral framework, focusing our attention on the possibility of a two-singularity scheme. A sort of hybrid model is proposed where both the usual multiperipheral kernel and the Pomeron singularity are coupled to the Reggeon dipole. We give reasons for expecting in this case a weak f and ω renormalization, even in SU(2). Using dual field theory as a guide, we discuss several problems related to the cylinder topology: overlap between clusters, daughter exchanges, signature and charge conjugation, and $t_{\min}$ cutoffs. Taking the two-particle s-channel discontinuity of the one-loop double-twisted graph, we show that the production of two overlapping clusters admits a sort of multiperipheral description where the overlap region is governed by the Pomeron singularity.

I. INTRODUCTION

In the last few years, a serious effort has been made in the framework of the topological expansion[1] to reach a semiquantitative understanding of the main features of strong-interaction physics: Regge trajectories, exchange-degeneracy breaking, Pomeron singularity, Zweig-rule violations, etc. Using multiperipheral schemes, numerical calculations have been carried out with very encouraging results.[2] In SU(2) we have at the planar level a set of four exchange-degenerate trajectories (ρ, ω, f, A_2). When the cylinder topology (Fig. 1) is introduced,[3] the f trajectory is boosted up and becomes the Pomeron, while the f and A_2 trajectories remain unchanged. A problem appears with the ω, which is shifted down or can even disappear, but the situation is improved by introducing broken SU(3) and realistic fits are possible[4,5] with the help of nonleading trajectories and thresholds.

The Pomeron-f identity implies the so-called "f extinction", i.e., we have only one singularity instead of a Pomeron plus an f. This is not the most pleasant solution from the point of view of dual field theory[6] (DFT) or quantum chromodynamics[7] (QCD), where in both cases one thinks of the Pomeron as a new singularity corresponding to a many-gluon state. Furthermore, as emphasized by Veneziano,[8] the Pomeron-f identity is not a necessary consequence of the topological expansion but rather of the multipheripheral hypothesis. In connection with the expansion in terms of N_c (the number of colors) and N_f (the number of flavors), Veneziano remarks that the widths of the resonances are proportional to $\rho = N_f/N_c$ and shows that only when $\rho \gg 1$ does one expect the mean cluster size to be small compared to the mean gap size and therefore the multi-Regge model to apply. When $\rho \ll 1$ one should rather consider the production of long-lived objects (massive clusters) cascading down to light particles. The real world seems to correspond to $\rho \sim 1$ and this suggests that both multiperipheral and heavy cluster components are to be taken into account. On the phenomenological level, the question of whether or not there are two high-lying $I^c = 0^+$ trajectories remains controversial[5,9] and there is no reason for discarding either of the two schemes.

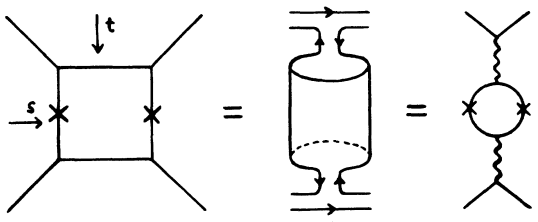

FIG. 1. The cylinder graph and topology.

The object of this paper is to discuss the problem of the f extinction and of the $C = -$ component renormalization going beyond multiperipheral dynamics. We present a systematic discussion of several points related to the cylinder topology such as overlap between clusters, contribution of daughter exchanges, signature projectors, charge conjugation, and $t_{\min}$ cutoffs. Both theoretical and phenomenological aspects are considered. In the theoretical part, DFT is used as a guide because (a) it provides the only precise formulation of mathematical duality; and (b) it can be regarded as the limit of some underlying field theory through fish-net diagrams. But, as the construction of completely satisfying dual amplitudes remains an unachieved goal, we focus our attention on qualitative features which are considered not to depend on the details of the theory. In particular, we do not wor-

ry about the precise values of intercepts, the number of dimensions, etc. We equally neglect logarithmic factors and therefore assume that the dual Pomeron is a pole. Given the fact that a new singularity appears, whose intercept does not depend on the Reggeon intercept, we are mainly interested in getting a qualitative understanding of the kinematical region of intermediate states from which this singularity is generated as well as the fundamental mechanism behind this result.

Section II deals with the phenomenological aspects: Concentrating on the possibility of a new Pomeron singularity higher than the f trajectory, we show that a compensation mechanism is expected for both the f and ω renormalization in which the multiperipheral boost and the repulsion by the Pomeron (or the $C=-$ Pomeron daughter) have opposite effects. Section III is devoted to the more theoretical aspects: Dynamical origin of the Pomeron in DFT, signature projectors, and charge conjugation. The analysis of intermediate states is done in Sec. IV where we study the contribution of each two-cluster kinematical configuration (considering as clusters the s-channel intermediate particles) to the one-loop cylinder graph in DFT, especially when both intermediate particles are heavy and, considered as composite or decaying objects, overlap in the rapidity plot. We show in Sec. V that the results lead to a new sum rule for the rapidity overlap region, which is dominated by the new Pomeron singularity, and to a new peripheral scheme in which planar clusters are redefined by cutting off the overlap region. To each of the new planar clusters there corresponds a finite-mass sum rule (FMSR), so that the picture looks very much like a conventional many-cluster scheme, with the peculiarity that now the "gap" is not empty, but filled by a two-cluster many-particle state (once the clusters decay). Section VI contains the conclusions. We include also an appendix with numerical calculations associated with Sec. II.

II. PHENOMENOLOGICAL ASPECTS

The phenomenological part of the discussion is done within a simple kinematical scheme: we are in a four-dimensional world, but the transverse momenta, although nonzero, are small compared to the longitudinal ones. This allows the use of typically two-dimensional approximations without neglecting the dynamical roles of transverse dimensions (which remain coupled through the polarizations of clusters and the transverse momenta of low-mass particles). Moreover, our analysis of intermediate states in DFT (Sec. IV) leads to results supporting such a kinematical approach. We can then handle the problem of overlapping clusters and discuss the phenomenological implications of non-multi-Regge effects in the overlap region, which, as we shall discuss, are related to nonleading exchanges.

Roughly speaking, we can distinguish two kinds of objects exchanged or produced. One is the leading trajectory and the produced resonances with $J=\alpha(s)$; the other is the nonleading exchanges and some "background" which in mathematical dual amplitudes is described by resonances with $J<\alpha(s)$. Let us represent the first kind (leading objects) by a full line [Fig. 2(a)] and the second kind by a full line accompanied by a dotted line [Fig. 2(b)]. In a quark model language, the dotted line would correspond to something like a radial excitation which increases the mass leaving the angular momentum unchanged. Although conventional finite-energy sum rules (with only leading objects) are a reasonable approximation for several phenomenological applications, it is well known since the detailed work of Ademollo *et al.*[10] that the leading Regge trajectories cannot bootstrap themselves. In particular mathematical duality requires not only leading objects but also nonleading ones, so that the duality equation can be represented as in Fig. 3 (with sums understood). At finite energies both kinds of objects add coherently and cannot be separated.

Analogously, a complete calculation of the box diagram implies putting both leading and nonleading objects in all internal lines. For instance, one has to include not only Fig. 4(a) (which contributes to the two-cluster multiperipheral term) but also Fig. 4(b) (in which the clusters exchange nonleading trajectories) or Fig. 4(c) (in which a "radial excitation" goes around the loop without being absorbed or produced by any vertex). The multiperipheral approximation amounts to neglecting Figs. 4(b) and 4(c).

When applied to production amplitudes the multiperipheral (multi-Regge) hypothesis permits a simple description in terms of clusters and gaps. Using quark diagrams, typical events are represented in Fig. 5(a). The quark lines emit particles or resonances which are ordered in rapidity and clusters are defined as groups of final-state objects between two consecutive crossed gaps. The rapidity gaps are supposed to be large enough to neglect nonleading exchanges, and the multi-Regge

FIG. 2. (a) Propagation of leading-trajectory states. (b) Propagation of daughter-trajectory states or, in general, nonleading objects.

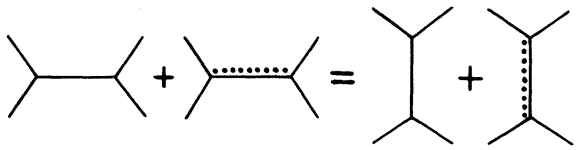

FIG. 3. Duality equation in terms of produced and exchanged leading and nonleading objects.

amplitudes are such that $t_{\min}$ effects suppress events characterized by massive overlapping clusters (see, for instance, Chan *et al.*, Ref. 2). In the unitarity sum, the multiperipheral states defined above build up the cylinder topology and, since the crossed loop acts as a twist operator on the quark lines of the t-channel Reggeon, the two-cluster term will be proportional to the charge-conjugation operator in the t channel (see Chew and Rosenzweig, Ref. 2). This means, once we write FMSR for clusters, that the Reggeon dipole will have equal weight and opposite signs for $C = \pm$. Consequently, in a world with SU(2), it is not possible to promote the f without lowering the ω trajectory. But crucial to this feature is the fact that in the multiperipheral approach the cylinder amplitude does not carry any "signature projector", unlike what happens in DFT (Refs. 11 and 12) as will be discussed in Sec. III.

In the J plane, one usually associates with the Reggeon propagator a factor $g_R/(J-\alpha_R)$ where α_R is the t-dependent Regge trajectory, and the cylinder is described by a factor k times (within the multiperipheral assumptions) the charge-conjugation operator. After iteration one has

$$A^C_{\text{singlet}} = \frac{g_R}{J-\alpha_R - Cg_Rk}\,, \tag{1}$$

where C is the charge-conjugation quantum number, i.e., the parity under the exchange of quark and antiquark lines. A way of attenuating the ω depression before breaking SU(3) is to give a suitable J dependence to g_R and k. Indeed, if g_Rk is a function of J with positive slope in the region of interest, we can in principle make compatible an important f promotion with a moderate ω lowering, and there are several ways of obtaining such a behavior for g_R and k.

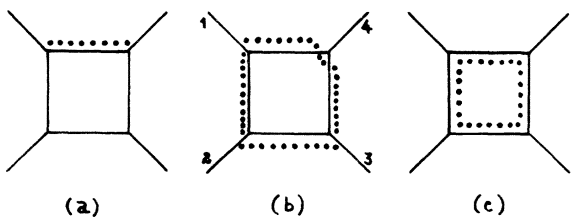

FIG. 4. Some graphs contributing to the whole one-loop planar diagram. (b) contains "radial excitations" propagating along internal lines between particle 1 and particle 2, between particle 2 and particle 3, and between particle 3 and particle 1.

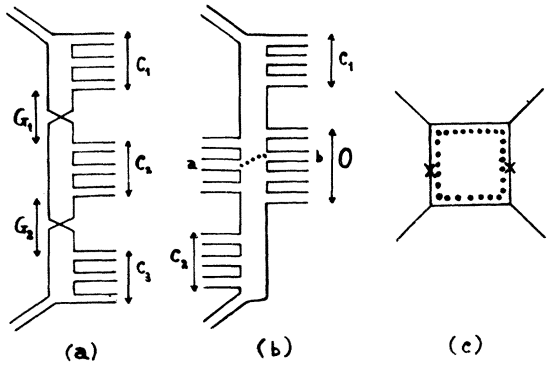

FIG. 5. (a) Conventional multiperipheral description of the n-particle intermediate states in terms of quark lines, clusters (C_i) and gaps (G_i). (b) An event which does not fit in the conventional scheme. O is the overlap region between particles emitted by both quark lines and the dotted line is a "radial excitation" traveling from particle a to particle b. (c) DFT description of the shadow of event (b).

One can, for example, modify the FMSR for clusters introducing daughters. This, together with SU(3) breaking, was used by Dash[5] to make compatible a Pomeron at 1.07 with an ω at 0.48, but it required very strong couplings for both the daughter trajectory and the leading $\lambda\bar{\lambda}$ state. Another way[13] is to add to the FMSR a low-energy term associated with high orders of the topological expansion, but the result achieved is not sufficient. Still a different way within the multiperipheral framework is proposed by Chan and Tsun and Webber,[14] who suggest that the mixing with $qq\bar{q}\bar{q}$ states coming from baryon amplitudes can boost up the ω trajectory.

An alternative approach is to assume that the cylinder graph generates by itself a new singularity with definite signature which dominates the exchange of vacuum quantum numbers. A nonleading $C = -$ component can also be included, following the results of DFT. Pinsky and Snider[9] attempted a fit along these lines and even neglected the usual multiperipheral terms. They obtained reasonable results in broken SU(3), with an output Pomeron at 1.06, an f at 0.40, and an f' at 0.12. In order to have $\alpha_\omega - \alpha_\rho < 0$, the Pomeron daughter was assigned negative residue and thought of as a cut rather than as a pole.

The motivation for going beyond multiperipheral schemes comes from the intermediate states with large multiplicity and small rapidity gaps. At small gaps nonleading exchanges become important and the Regge approximation is not a good description of such events. More precisely, let us con-

sider the diagram of Fig. 5(b). We see that there is a region where we cannot organize the produced particles in planar clusters separated by reasonable gaps. In this region of the diagram it is not possible to neglect daughter exchanges such as the radial excitation circulating between particle a and particle b, whose shadow, in the language of DFT, would lead for the one-loop amplitude to the process depicted in Fig. 5(c). The most natural way of treating Fig. 5(b) is perhaps to consider two planar clusters (C_1 and C_2) and an "overlap region" O where both quark lines emit particles. For C_1 and C_2 one would write Reggeon sum rules while to the "overlap" O one has to associate, besides the conventional multiplipheral term, a new object whose properties cannot be determined from a multiperipheral scheme. This would also have consequences for signature and charge conjugation. For instance, let us consider the structures of Figs. 6(a) and 6(b), which both lead to the cylinder of Fig. 6(c), and the structure of Fig. 7(a) leading to the cylinder of Fig. 7(b). In Fig. 6(a), the two planar clusters exchange a leading Reggeon while in Fig. 6(b) they are separated by a two-cluster overlap. Figure 7(a) is similar to Fig. 6(b) and leads to the cylinder structure of Fig. 7(b). Figure 6(a) can be included in the conventional approach with FMSR and Reggeon exchanges. Figures 6(b) and 7(a) correspond to something new. In particular, if we write their contributions to the shadow scattering in a completely factorized way (cluster $\times$ overlap $\times$ cluster = Reggeon $\times$ new object $P_0 \times$ Reggeon), we get a Reggeon dipole times some new function of J which accounts for the structure of P_0. In the limit where such a factorized description would be correct, Figs. 6(b) and 7(a) would contribute with the same weight to the Reggeon dipole. This is what happens in the approach used by Hong Tuan[15,16] for the Pomeron singularity, which is based on this kind of diagrams. In such a factorizable limit, the new dipole term has identically $C=+$ as can be seen adding the quark contents of Figs. 6(c) and 7(b), and is an acceptable candidate for carrying the Pomeron pole. If one wants to be more accurate and relax the factorization condition, one can add a nonleading $C=-$ component and we get close to the Pinsky-Snider scheme. In Secs. III and IV, we shall give precise theoretical arguments based on DFT which justify this kind of approach provided that the new $C=+$ singularity is higher than the Reggeon.

In fact, a complete approach should take into account both the new object P_0 and the multiperipheral component. In DFT, they come from different critical points in the integral expression of the twisted box diagram and correspond to different kinematical regions of the s-channel intermediate

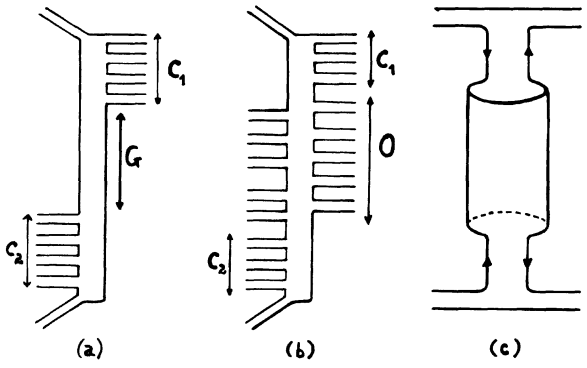

FIG. 6. (a) Multiperipheral contribution to the Pomeron dipole. (b) Nonmultiperipheral term carrying the same internal quantum numbers. (c) Topological and quark-line description of the shadow of both events (omitting holes).

states. These points will be discussed in detail in Secs. IV and V. It is then natural to write for the cylinder

$$K^C = Ck + \frac{\delta_C}{J - \alpha_C}\,, \tag{2}$$

where C is the charge conjugation, $\alpha_+ = \alpha_{P_0}$, and $\alpha_- = \alpha_{P_0} - 1$. δ_+ and δ_- are the couplings of the Reggeon to the Pomeron and to its $C=-$ daughter. For k, δ_+, δ_- positive and $\alpha_{P_0} > \alpha_R$, and assuming exact SU(2), we note the following: For the f renormalization, the multiperipheral component is positive and the Pomeron mixing is negative. The opposite happens to the ω: The multiperipheral term tends to depress it while, because $\alpha_\omega - \alpha_{P_0} + 1$ is positive, the Pomeron daughter pushes it up. In particular, both the f and the ω trajectories remain unrenormalized if one has

$$\delta_+ = (\alpha_{P_0} - \alpha_R)k\,, \tag{3a}$$

$$\delta_- = (1 + \alpha_R - \alpha_{P_0})k\,. \tag{3b}$$

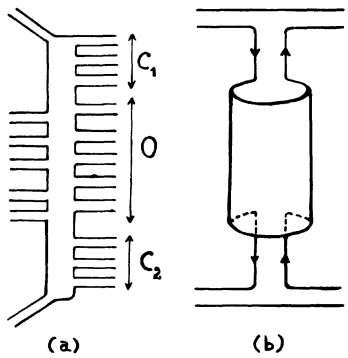

FIG. 7. (a) Another possible nonmultiperipheral contribution to the Pomeron dipole. (b) Topological and quark-line description of the shadow of this event (omitting holes).

This result remains true in broken SU(3). For the residues, the derivatives of K^c at $J=\alpha_R$ will induce renormalization effects. In broken SU(3), both f' and ϕ will receive a component with nonstrange quarks (thus allowing for Okubo-Zweig-Iizuka rule violations), but the f and ω poles will remain free of mixing if Eqs. (3a) and (3b) hold true. In general, Eqs. (3a) and (3b) have no reason to be satisfied but the tendency towards a compensation between the multiperipheral and the Pomeron components will always give a smaller f renormalization than if we have only the repulsive Pomeron mixing. Something similar happens to the ω. Note also that if one wants to obtain $\alpha_\omega < \alpha_\rho$, it is enough to take $k > \delta_-/(1+\alpha_R-\alpha_{P_0})$ and the residue of the Pomeron daughter has no reason to be negative.

Both components of the cylinder come from the same set of graphs of DFT and we expect them to have the same behavior in terms of N_f and N_c. More precisely, following the analysis of Ref. 8, one has

$$k \sim \delta_+ \sim \delta_- \sim \rho = \frac{N_f}{N_c} \quad \text{for } \rho \ll 1, \tag{4a}$$

$$k \sim \delta_+ \sim \delta_- \sim 1 \quad \text{for } \rho \gg 1. \tag{4b}$$

For $\rho \sim 1$ (which seems to happen in the physical world), the situation is intermediate between both limits. It is then likely that the parameters under consideration will have moderate values and the compensation mechanism will favor weakly renormalized f and ω trajectories, even without the help of broken SU(3) (or with small $\lambda\bar{\lambda}$ components when the third quark is introduced).

What other experimental consequences would such a picture imply? The absence of multiperipheral constraints leads to the production of heavy clusters whose effect should be detected by particle correlation measurements, especially in high-multiplicity events. Measurements of two-particle semi-inclusive correlations at ISR energies in pp reactions[17] allowed the determination of the ratio $A_{n_c} = \langle m \rangle_{n_c} / \langle m(m-1) \rangle_{n_c}$ of the first and second moments of the charged multiplicity distribution of the cluster decay as observed in events of fixed charged multiplicity n_c. The most popular models for particle production favor low-multiplicity clusters with a narrow decay distribution leading for A_{n_c} to a flat or slowly rising n_c dependence. The data follow this picture for $n_c < 1.5$ to $2\langle n_c \rangle$ but show a much more rapid rise in n_c above this value. This is compatible with the production of heavier objects becoming important in high-multiplicity reactions. Heavy clusters could also be looked for by analyzing the rapidity interval distributions[18] with a fixed number of particles in the interval. Data for pp scattering between 70 and 200 GeV (Ref. 19) seem to require heavy clusters decaying into six to eight pions in order to obtain a good fit.[20] There have been also claims in favor of two-cluster schemes[21] which are compatible with data at present energies. But the question remains open and we do not want to make any statement here.

We conclude this section with a comment on baryon loops. As before we will have a multiperipheral and a Pomeron component. The former is expected to renormalize both the f and the ω upwards[14] whereas the latter will give two differnt $C=+$ and $C=-$ components, as for the meson loop. From the point of view of rapidity space a pure multiperipheral scheme would be even less justified than for meson loops, since in that case a rough estimate of the average gap size will give

$$\langle Y_g \rangle_{\text{baryons}} \simeq \frac{1}{\alpha_f - 2\alpha_B + 1} \sim \tfrac{1}{2} \langle Y_g \rangle_{\text{mesons}}$$

(α_f and α_B are the conventional renormalized f and the baryon trajectories, respectively) while the average cluster size is, just as for mesons,

$$\langle Y_{\text{cl}} \rangle \simeq \frac{1}{\alpha_f - \alpha_R},$$

which strongly increases the frequency of events with overlapping clusters and in general enhances the corrections to the Regge approximation.

III. THEORETICAL ASPECTS

In DFT,[6] we have the well-known infinite set of four-vector operators $a_\mu^{(n)}$, $n \geq 1$ which, when coupled to the external momenta, generates the wave function of the N-particle intermediate states. The successive powers of $a_\mu^{(1)}$ generate the exchange-degenerate leading trajectory, while the $a_\mu^{(n)}$'s, $n \geq 2$ carry radial excitations which increase the mass of the produced particles and originate in this way the daughter trajectories required by mathematical duality.

Using the integral representation, we can write the box-diagram amplitude for four external particles as

$$F(p_1,p_2,p_3,p_4) = \int_0^1 dx_1 dx_2 dx_3 dx_4 \times \int dk \prod_i x_i^{-\alpha(k_i^2)-1} T(x_i, p_i), \tag{5a}$$

with

$$T(x_i,p_i) = \mathrm{Tr}[x_1^{-H} V(p_1) x_2^{-H} V(p_2) x_3^{-H} \times V(p_3) x_4^{-H} V(p_4)], \tag{5b}$$

where the p_i's are the momenta of the external particles, the k_i^2's are the squared momenta of

internal lines, $\int dk$ means integration over all dimensions of space and time, $V(p_i)$ is the vertex operator for particle i, and $H = h_0 + \sum_{n,\mu} n a_\mu^{(n)\dagger} a_\mu^{(n)}$. h_0 is a mass operator related to the mass of the ground state. For more details, we refer the reader to Ref. 6.

Expression (5b) corresponds to the planar diagram of Fig. 4. When twists are introduced as in Fig. 1, the only difference is that twist operators appear in the trace. A common feature is that radial excitations which go around the loop as in Figs. 4(c) or 5(c) induce powers of $\omega = x_1 x_2 x_3 x_4$ in the integrand of (5a). When the sum over all oscillation modes is performed as in Ref. 22, one gets a factor $f(\omega)^{-d}$, where

$$f(\omega) = \prod_{n=1}^{\infty} (1 - \omega^n) \tag{6}$$

and d is the number of space-time dimensions. Actually, in models with gauge identities one gets $f(\omega)^{-(d-E)}$, where E is the number of decoupled dimensions [$E = 2$ for $\alpha(0) = 1$, $d = 26$]. In the nonplanar case one obtains besides of this factor, a power $f(\omega)^{-\bar{\alpha}(t)}$ where the slope of $\bar{\alpha}(t)$ is half of the slope of the input Regge trajectory. The exponential divergence of $f(\omega)^{-1}$ near $\omega = 1$ gives the well-known divergence of the planar loop (which has to be removed by an adequate renormalization procedure[23]), while in the double-twisted diagram the t dependence of the exponent of $f(\omega)$ gives rise to a new Regge trajectory. In both cases we have a collective effect of all daughter trajectories which propagate along *all* internal lines, so that if we select leading Reggeons in just one of the internal lines (and, in particular, among the objects exchanged between clusters), we are automatically cutting off any phenomenon of this kind.

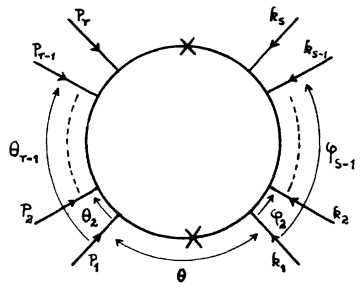

FIG. 8. N-particle one-loop cylinder diagram ($N = r + s$).

One of the most important features of the new singularity is that it carries signature projectors, which allow it to be interpreted as the Pomeron. Such projectors where already found at each critical point by Alessandrini, Amati, and Morel[11] in the calculation of the asymptotic behavior of the four-particle double-twisted box diagram. Also Cremmer and Scherk[12] found signature projectors in the N-particle operator formalism they constructed to factorize in the t channel the residues of the new poles. Here we shall discuss the asymptotic behavior at fixed t of the N-particle amplitude ($N = 4$ is not enough because we would miss, for instance, the $C = -$ component).

The cylinder amplitude corresponding to the topology of Fig. 8 is given by[12]

$$\tilde{F}_{r,s} = g(t) \int_0^1 dq\, q^{-1-\alpha_P(t)} h(q) \int_0^{\pi} d\theta \int \prod_{i=2}^{r} d\theta_i \prod_{l=2}^{s} d\varphi_l \times \prod_{i<j} \bar{\psi}(\theta_j - \theta_i)^{-2\alpha' p_i \cdot p_j} \prod_{l<m} \bar{\psi}(\varphi_m - \varphi_l)^{-2\alpha' k_m \cdot k_l} \times \prod_{i,l} \bar{\psi}_T(\theta + \theta_i + \varphi_l)^{-2\alpha' p_i \cdot k_l} , \tag{7}$$

with

$$\bar{\psi}(\theta) = \sin\theta \prod_{n=1}^{\infty} \frac{1 - 2q^{2n}\cos 2\theta + q^{4n}}{(1 - q^{2n})^2} , \tag{8a}$$

$$\bar{\psi}_T(\theta) = \prod_{n=1}^{\infty} \frac{1 - 2q^{2n-1}\cos 2\theta + q^{4n-2}}{(1 - q^{2n})^2} , \tag{8b}$$

$$0 = \theta_1 \leq \theta_2 \leq \cdots \leq \theta_r \leq \pi , \quad 0 = \varphi_1 \leq \varphi_2 \leq \cdots \leq \varphi_s \leq \pi$$

$$t = (p_1 + p_2 + \cdots + p_r)^2 = (k_1 + k_2 + \cdots + k_s)^2 ,$$

$$\ln q = 2\pi^2 / \ln \omega .$$

$h(q)$ is related to $f(\omega)$ and is such that $h(q) - 1$ behaves like q^2 in the limit $q \to 0$, i.e., $\omega \to 1$. α' is the slope of the input Regge trajectory $\alpha(t)$, and $\alpha_P(t)$ the dual-Pomeron trajectory. We do not worry about intercept problems here. For the θ variables and other details, see Refs. 6 and 12.

If we are interested only in the leading singularity and the first daughter, we can expand in powers of q and make some approximations:

$$\bar{\psi}(\theta) \sim \sin\theta ,$$

$$\bar{\psi}_T(\theta) \sim \exp(-2q\cos 2\theta - 2q^2\cos^2 2\theta + 3q^2) ,$$

$$h(q^2) \sim 1 , \quad q \to 0 .$$

The kinematical limit of interest is

$$2\alpha' p_i \cdot k_l = \epsilon_i \delta_l s + \omega_{il} , \quad s \to \infty \text{ and } \epsilon_i, \delta_l, \omega_{il} \text{ fixed} \tag{9a}$$

with

$$\sum_i \epsilon_i = \sum_l \delta_l = 0 . \tag{9b}$$

The product of the $\bar{\psi}_T$'s can then we written as

$$\sum_{i,l} \psi_T(\theta + \theta_i + \varphi_l)^{-2\alpha' p_i \cdot k_l} \sim \exp\left[2q \sum_{i,l} [\cos 2(\theta + \theta_i + \varphi_l) + q\cos^2 2(\theta + \theta_i + \varphi_l)](\epsilon_i \delta_l s + \omega_{il})\right]$$

$$\sim e^{\mu}\left(S_+ + \frac{1}{s} S_-\right) , \tag{9c}$$

with

$$S_+ = 1 \quad \text{and} \quad S_- = \mu \frac{\sum_{i,l} \omega_{il} \cos 2(\theta + \theta_i + \varphi_l)}{\beta \cos 2(\theta + \bar{\theta})} + \mu^2 \frac{\sum_{i,l} \epsilon_i \delta_l \cos^2 2(\theta + \theta_i + \varphi_l)}{\beta^2 \cos^2 2(\theta + \bar{\theta})} ,$$

where we have made the change of variables

$$\mu = 2qs\beta \cos 2(\theta + \bar{\theta}) . \tag{10a}$$

$\beta(\theta_i, \varphi_l)$ and $\bar{\theta}(\theta_i, \varphi_l)$ are defined by:

$$\beta \cos\bar{\theta} = \sum_{i,l} \epsilon_i \delta_l \cos(\theta_i + \varphi_l) ,$$

$$\beta \sin\bar{\theta} = \sum_{i,l} \epsilon_i \delta_l \sin(\theta_i + \varphi_l) . \tag{10b}$$

We then obtain

$$\tilde{F}_{r,s} \sim g(t)[R_+ s^{\alpha_P(t)} + R_- s^{\alpha_P(t)-1}] , \tag{11a}$$

where

$$R_\pm = \int \prod_{i=2}^{r} d\theta_i \prod_{l=2}^{s} d\varphi_l \prod_{i<j} \sin(\theta_i - \theta_j)^{-2\alpha' p_i \cdot p_j} \prod_{l<m} \sin(\varphi_m - \varphi_l)^{-2\alpha' k_m \cdot k_l} \beta^{\alpha_P(t)}$$

$$\times \int_0^\infty d\mu\, \mu^{-\alpha_P(t)-1} e^{-\mu} \int_0^\pi d\theta [\cos 2(\theta + \bar{\theta})]^{\alpha_P(t)} S_\pm . \tag{11b}$$

The expression $\cos 2(\theta + \bar{\theta})$ is periodic in θ of period π and changes sign under the transformation $\theta \to \theta \pm \pi/2$. To do the θ integration we split the interval into two pieces: one-half period where $\cos 2(\theta + \bar{\theta})$ is positive, the other half period where it is negative, which yields the phase $e^{-i\pi\alpha_P(t)}$. The net result is the signature factor $(1 + e^{-i\pi\alpha_P(t)})$ which projects out positive signature for S_+ and negative signature for S_-.

When SU(N) is introduced via the Chan-Paton procedure, charge conjugation corresponds to the twist operator. Assuming that the external scalar particles belong to a multiplet with $C = +$, the parity under twist is equal to the parity under charge conjugation provided the Chan-Paton formula is used. It is then easy to see that the relevant transformation for expression (7) is

$$\theta + \theta_i + \varphi_l \to \theta + \theta_i - \varphi_l$$

inside the $\bar{\psi}_T$ functions, the rest of the integrand remaining unchanged. This gives $\beta^2(\theta_i, \varphi_l) = \beta^2(\theta_i, -\varphi_l)$ which, for R_+, is enough to ensure positive charge conjugation at all t, taking into account that one has to integrate over both signs of

$\cos 2(\theta+\bar{\theta})$. Integrating over $d\theta$ and using (9b), the term proportional to μ^2 in S_- disappears at $\alpha_P(t)=2$ and contributes only to $C=-$ for other values of t. The term which contains the ω_{ij}'s gives a mixture of both C's and the $C=+$ component is related to the timelike component of the leading term in the t channel.

The residue of the Reggeon dipole can be analyzed using the same procedure. For this, one has to consider the limit in which all θ_i and all φ_l tend to zero or π. The result is consistent with the residue obtained in Ref. 11, which has the form

$$\tilde{\Sigma}(t)=\gamma g^2\int_0^{\pi}d\theta\int_0^1 dq\, q^{-1-\alpha_P(t)}h_R(q^2)\times g(\theta,t)V(q,\theta)^{\alpha_R(t)}\,, \tag{12a}$$

with

$$V(q,\theta)=-2\sum_{m=1}^{\infty}m\,\frac{q^m}{1-q^{2m}}\cos 2m\theta \tag{12b}$$

and, considering the zeros of $V(q,\theta)$ in the integration region, we can see that, in fact $\tilde{\Sigma}(t)$ splits into two separate residues, one for each signature:

$$\tilde{\Sigma}_{\pm}(t)=\gamma g^2\int_0^1 dq\, q^{-1-\alpha_P(t)}h_R(q^2)\Delta_{\pm}(q,t)\,, \tag{13a}$$

with

$$\Delta_{\pm}(q,t)=\int_0^{\pi}d\theta\,|V(q,\theta)|^{\alpha_R(t)}g(\theta,t)\times\{\theta[V(q,\theta)]\pm\theta[-V(q,\theta)]\}\,, \tag{13b}$$

where plus signature corresponds to $C=+$ and minus signature to $C=-$.

Daughter trajectories are also important in the planar loop: omitting them one eliminates a part of the leading-trajectory renormalization and perhaps of the massive-cluster contribution. But in this case the integration over the θ variable does not play the same role as for $\tilde{\Sigma}(t)$ and we do not expect signature projectors to appear.

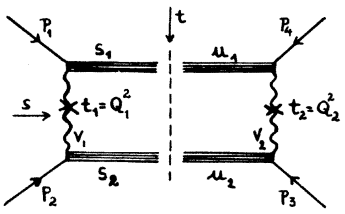

FIG. 9. Kinematics for the factorization in terms of two-massive-particle (or two-cluster) intermediate states. s_1 and s_2 are the squared masses of the intermediate objects, and Q_1 and Q_2 are the momenta of the exchanged twisted Reggeons. All external momenta are taken to be incident.

IV. THE STRUCTURE OF THE INTERMEDIATE STATES

The four-particle nonplanar orientable one-loop amplitude can be written as[6]

$$\tilde{F}(p_1,p_2,p_3,p_4)=\int dQ_1\Phi(s,s_i,t_j)\,, \tag{14}$$

with

$$\phi(s,s_i,t_j)=\int du_1du_2dv_1dv_2v_1^{-\alpha(t_1)-1}v_2^{-\alpha(t_2)-1}u_1^{-\alpha(s_1)-1}u_2^{-\alpha(s_2)-1}(1-u_1)^{-\alpha(t)-1}(1-u_2)^{-\alpha(t)-1}$$
$$\times\left(\prod_{n=1}^{\infty}(1-\omega^n)\right)^{-12\alpha_P(t)}\exp\left(\alpha' s\sum_{n=1}^{\infty}(-1)^n\,\frac{(1-u_1^n)(1-u_2^n)(v_1^n+v_2^n)}{n(1-\omega^n)}\right)\tilde{f}(u_i,v_j,t)\,, \tag{15}$$

where $\omega=u_1u_2v_1v_2$. $\tilde{f}(u_i,v_j,t)$ contains factors irrelevant for our purposes and we set it equal to a constant. The notations are defined in Fig. 9: The u_i variables correspond to the (untwisted) cluster lines which carry momenta P_i and squared masses s_i, while the v_j variables are associated to the twisted Reggeons of momenta Q_j and squared momenta t_j. The integration is made in the region

$$0\le u_i\le 1\,,\quad 0\le u_iv_1v_2\le 1\,,\quad i=1,2\,;$$
$$\ln\omega\le\ln v_1-\ln v_2\le-\ln\omega\,.$$

The overall energy squared is $s=(p_1+p_2)^2$ and we are only interested in the case when the overall momentum transfer squared $t=(p_1-p_4)^2$ is 0 so that $Q_1=Q_2=Q$ and $t_1=t_2=\tilde{t}$. As already mentioned in Sec. III we do not specify the number of transverse dimensions since the calculations will show it is not important for our conclusions. $\alpha(t)$ and $\alpha_P(t)$ are the trajectories of the Reggeon and the Pomeron, respectively.

The crossed dual-loop amplitude has been studied in great detail by Alessandrini *et al.*[11] Following previous works, they first performed the loop mementum integration $\int dQ$ and then showed that the integral in u_i and v_j could be evaluated by considering the behavior of the integrand at some critical points in the space

of variables u_i, v_j. They thus identified two pieces: the f-renormalization part corresponding to $u_i \sim 1$ but $\omega \sim 0$, and the Pomeron part arising when $\omega \sim 1$. What we would like to show here is that each of these regions in the u_i, v_j space is related to a different region of the phase space of the intermediate states. So unlike previous works we do not perform the loop momentum integration but rather study the integrand (15) for fixed values of the invariants s_i and $\tilde{t}$. We consider two separate regions:

(a) the region $s_i, s \to \infty$, $s/s_1 s_2 = \gamma \to \infty$ which, as expected, builds up the multiperipheral f renormalization.

(b) the region $s_i, s \to \infty$, $s/s_1 s_2 \to 0$ which generates the Pomeron.

A. The f renormalization

The limit of interest is $s_1 \to \infty$, $s_2 \to \infty$ for fixed $\tilde{t}$. Using standard techniques, we can deform the integration contour and expand around $u_1 = 1$ and $u_2 = 1$. Then, with the change of variables $\mu_i = -s_i(1-u_i)$, we get

$$\Phi \simeq G s_1^{\alpha(0)} s_2^{\alpha(0)} \int_0^{-\infty} d\mu_1 d\mu_2 (\mu_1\mu_2)^{-\alpha(0)-1} e^{\mu_1+\mu_2} \int dv_1 dv_2 (v_1 v_2)^{-\alpha(\tilde{t})-1} \exp[-\alpha' \gamma \mu_1 \mu_2 (v_1+v_2)/(1-v_1 v_2)] . \quad (16)$$

By analyticity $\mathrm{Im}\Phi$ has the same asymptotic behavior. Because of the exponential damping, only the finite values of μ_i are important in the integration, which implies $u_1, u_2 \simeq 1$. For large values of γ (which correspond to $\tilde{t}_{\min} \simeq 0$), and assuming $2\alpha(\tilde{t}) > \alpha(0)$, the region $v_1, v_2 \simeq 0$ brings a factor $\gamma^{2\alpha(\tilde{t})}$ which completes the multiperipheral behavior. But, for finite γ, the above Regge approximation does not apply while the factor $(s_1 s_2)^{\alpha(0)}$ (which generates the f-ω dipole when the Mellin transform is performed) is always there. This gives rise to nonmultiperipheral contributions to the Reggeon dipole.

When $\gamma \to 0$ (i.e., when clusters overlap), an exponential cutoff in $\tilde{t}$ appears (as in Chan *et al.*[2]), except near $v_1 v_2 = 1$. This is in fact the region where we expect the new singularity to appear. In order to study what happens, we come back to the original expressions and change our approximations.

B. The Pomeron

We first rewrite the integrand in Eq. (14) in terms of variables more suited to our purposes. Following Ref. 6 one finds

$$\left(\prod_{n=1}^{\infty}(1-\omega^n)\right)^{-12\alpha_P(t)} \exp\left(\alpha' s \frac{\sum_{n=1}^{\infty}(-1)^n(v_1^n+v_2^n)(1-u_1^n)(1-u_2^n)}{n(1-\omega^n)}\right)$$

$$= q^{-\alpha_P-1} \exp\left(\alpha' s \frac{(\ln^2 v_1 + \ln^2 v_1 u_1 u_2 - \ln^2 u_1 v_1 - \ln^2 u_2 v_1)}{2\ln\omega}\right)\left(\frac{\theta_4(\ln v_1/\ln\omega)\theta_4(\ln v_1 u_1 u_2/\ln\omega)}{\theta_4(\ln u_1 v_1/\ln\omega)\theta_4(\ln u_2 v_1/\ln\omega)}\right)^{-\alpha' s}, \quad (17)$$

where one has introduced the notation

$$\ln q = \frac{2\pi^2}{\ln\omega} ,$$

and the θ_4's are Jacobi functions.

As in Cremmer and Sherk[12] one defines the angular variables

$$\theta = \pi \frac{\ln v_1}{\ln\omega}, \quad \varphi = \pi \frac{\ln u_1}{\ln\omega}, \quad \text{and} \quad \eta = \pi \frac{\ln u_2}{\ln\omega}, \quad 0 \le \theta, \varphi, \eta \le \pi \quad (18)$$

and writes the right-hand side of Eq. (17) as

$$q^{-\alpha_P-1} e^{\alpha' s 2\eta\varphi/\ln q} e^{-\alpha' s V_s} , \quad (19)$$

where V_s is defined by[11]

$$V_s = \ln\left(\frac{\theta_4(\theta/\pi)\theta_4[(\theta+\varphi+\eta)/\pi]}{\theta_4[(\theta+\varphi)/\pi]\theta_4[(\theta+\eta)/\pi]}\right) = \sum_{p=1}^{\infty} \frac{1}{p} \frac{q^p}{1-q^{2p}} \sin p\varphi \sin p\eta \cos p(2\theta+\eta+\varphi) . \quad (20)$$

V_s is regular and vanishes at $q=0$.

On the other hand one notices[6] that the phase-space integral

$$\int dQ \prod_{j=1}^{2} v_j^{-\alpha(\tilde{t})-1} \prod_{i=1}^{2} u_i^{-\alpha(s_i)-1}$$

gives a factor $e^{-\alpha' s 2\eta\varphi/\ln q}$ which exactly cancels a similar term in expression (19) thereby allowing the Pomeron singularity to be generated, in the integration over q, by the $q \sim 1/s$ region. The Pomeron will

thus come from the values of the invariants s_1, s_2, and $\tilde{t}$ which dominate the phase-space integral. To find this kinematical region we write

$$\int dQ \prod_{j=1}^{2} v_j^{-\alpha(\tilde{t})-1} \prod_{i=1}^{2} u_i^{-\alpha(s_i)-1} \sim \int dQ \exp\left\{-\ln\omega\left[Q^2 + 2\,\frac{Q}{\pi}\,(p_1\varphi - p_2\eta)\right]\right\}, \tag{21}$$

with $s_1 = (p_1 + Q)^2$ and $s_2 = (p_2 - Q)^2$. The maximum of the integrand is reached at $Q = Q^I$ with

$$\pi Q^I = p_2\eta - p_1\varphi\,. \tag{22}$$

If we go to the center-of-mass frame, the value Q^I above has no transverse components, supporting our previous claim that we do not need to specify the number of space-time dimensions. Keeping only the longitudinal components we write

$$p_1 = (p, p), \quad p_2 = (p, -p),$$

and introduce the parameters λ and μ via

$$Q = (Q_0, Q_1) = p(\mu, -\lambda).$$

Then one finds:

$$\begin{aligned} &s_1 = \frac{s}{4}\,(\mu+\lambda)(2-\lambda+\mu), \quad s_2 = \frac{s}{4}\,(\lambda-\mu)(2-\lambda-\mu), \\ &Q^2 = \frac{s}{4}\,(\mu+\lambda)(\mu-\lambda), \quad \gamma = \frac{s}{s_1 s_2} = \frac{4}{s(\lambda+\mu)(\lambda-\mu)(2-\lambda+\mu)(2-\lambda-\mu)} \end{aligned} \tag{23}$$

with the kinematical constraints

$$0 \leq \lambda \leq 2 \quad \text{and} \quad |\mu| \leq 1 - |1-\lambda|\,.$$

Equation (22) splits into the following two conditions:

$$\eta = \pi\,\frac{\lambda+\mu}{2} = \eta_0 \quad \text{and} \quad \varphi = \pi\,\frac{\lambda-\mu}{2} = \varphi_0\,. \tag{24}$$

In consequence, to get the contribution to Eq. (14) of the kinematical region under study, we evaluate Eq. (14) integrating over q and θ, keeping η and φ at the values above. We get, neglecting transverse components,

$$\begin{aligned} \tilde{F}(p_1, p_2, p_3, p_4) &\sim \int dQ_0 dQ_1 \delta(Q_0 - Q_0^I)\delta(Q_1 - Q_1^I) dq d\theta d\eta d\varphi\; q^{-\alpha_P(0)-1} e^{-\alpha' s V_S} [(1 - e^{2\pi\varphi/\ln q})(1 - e^{2\pi\eta/\ln q})]^{-\alpha(0)-1} \\ &\sim \frac{1}{s^2} \int ds_1 ds_2 J\left(\frac{s_1}{s}, \frac{s_2}{s}\right) dq d\theta q^{-\alpha_P(0)-1} e^{-\alpha' s V_S(q,\theta,\varphi_0,\eta_0)} [(1 - e^{2\pi\varphi_0/\ln q})(1 - e^{2\pi\eta_0/\ln q})]^{-\alpha(0)-1} \end{aligned} \tag{25}$$

where J/s^2 comes from the integration over η and φ and from the change of variables (Q_0, Q_1) to variables (s_1, s_2). J behaves like a constant in the limit $s_1/s,\ s_2/s \to 0$, the exact form being irrelevant for our purposes. Performing the integration over q and keeping in mind that the region $q \sim 1/s$ dominates due to the exponential factor in the integrand of Eq. (25) we find

$$\tilde{F}(p_1, p_2, p_3, p_4) \sim \frac{1}{s_2} \int ds_1 ds_2 J\left(\frac{s_1}{s}, \frac{s_2}{s}\right) (\alpha' s \sin\varphi_0 \sin\eta_0)^{\alpha_P(0)} (\eta_0\varphi_0)^{-\alpha(0)-1} \int_0^{\pi} d\theta [\cos(2\theta + \varphi_0 + \eta_0)]^{\alpha_P(0)}. \tag{26}$$

As seen in Sec. III, the integration over θ gives the signature factor. From Eq. (26) one easily obtains the discontinuity ImA across the unitarity cut at fixed s_1, s_2 with the definition $\mathrm{Im}\tilde{F} = \int ds_1/s_1 (ds_2/s_2)\mathrm{Im}A$. There are several cases of interest:

$$\begin{aligned} &\text{(a)}\ \frac{s_1}{s}, \frac{s_2}{s}\ \text{constant}, \quad \frac{s_1 s_2}{s} \to \infty, \\ &\mathrm{Im}A \sim F\left(\frac{s_1}{s}\right) F\left(\frac{s_2}{s}\right) \left(\frac{s_1 s_2}{s}\right)^{\alpha_P(0)}; \end{aligned} \tag{27}$$

$$\begin{aligned} &\text{(b)}\ \frac{s_1}{s}, \frac{s_2}{s} \to 0, \quad \frac{s_1 s_2}{s} \to \infty, \\ &\mathrm{Im}A \sim \left(\frac{s}{s_1}\right)^{\alpha(0)} \left(\frac{s}{s_2}\right)^{\alpha(0)} \left(\frac{s_1 s_2}{s}\right)^{\alpha_P(0)}. \end{aligned} \tag{28}$$

The two expressions above give the contribution, to the unitarity equation, of the production of two massive objects in the limit when $s_1 s_2/s \to \infty$.

Before discussing the meaning of these formulas we make a comment on the size of transverse

components. Q_T^2, the square of the transverse momenta of the intermediate particles grows, according to Eq. (21), with s like

$$Q_T^2 \sim -\frac{1}{\ln\omega} \sim -\ln q \sim \ln\gamma , \tag{29}$$

whereas the masses themselves grow at least like $1/\gamma$. This result is consistent with the usual picture, well supported experimentally, where decay products of a hadronic mass M are emitted with a limited transverse momentum and with multiplicity increasing like $\ln M$. This point is important to justify the following discussion in terms of rapidity variables.

V. DISCUSSION AND INTERPRETATION

It is interesting to observe that the results of Eqs. (27) and (28) have a form similar to a two-cluster Regge amplitude. In order to make this analogy explicit we go to the rapidity formalism, which is convenient to discuss hadronic reactions where there is a cutoff in transverse momentum. In this picture, an unstable cluster of mass M, decaying into secondaries of mass m, occupies a certain length in the rapidity phase space defined by $M^2 = (m^2 + p_T^2)e^y$, where p_T is the (limited) average transverse momentum of decay products. In the graph we considered, heavy particles are stable, a feature which is clearly unphysical. However, we saw that their transverse properties are compatible with those of hadronic masses decaying into particles of limited transverse momenta. We therefore feel justified in using the rapidity language. Dropping the irrelevant $(m^2 + p_T^2)$ factors we then associate a width in the rapidity plot to a cluster of mass squared s_i via (see Fig. 10)

$$Y_i = \ln s_i , \quad Y = \ln s ,$$

while the "overlap" between the clusters is $Y_0 = Y_1 + Y_2 - Y = \ln(s_1 s_2/s)$. If we denote $y_1 = Y - Y_2$, $y_2 = Y - Y_1$, and $y_0 = Y_0$, Eq. (28) becomes

$$\mathrm{Im}A \sim e^{y_1\alpha(0) + y_2\alpha(0) + y_0\alpha_P(0)} . \tag{30}$$

The analogy with the usual peripheral expression is obvious: The usual gap between clusters is replaced by the overlap of size y_0 and the cut $\alpha_{\mathrm{cut}} = 2\alpha - 1$ by the Pomeron α_P. The "clusters" c_1 and c_2 are obtained from the original ones C_1 and C_2 by truncation of the overlap region (see Fig. 10). It is remarkable that the dual model for the production of two stable clusters suggests an interpretation such as that depicted in Fig. 10. Narrow particles split without decaying and rearrange giving a sort of multiperipheral scheme with new effective planar clusters and a Pomeron dominated kernel which corresponds to the overlap between the narrow particles treated as extended clusters. Even in the case $N_F/N_c \ll 1$, when widths are small and one would expect the right picture to be direct channel production of two overlapping clusters, formula (28) shows that in fact a sort of multiperipheral order dominates. We can say that the underlying dynamics sees the composite nature of the produced massive particles, not just in terms of the many-particle states in which they will decay, but through something which is already present at the zero-width approximation (the vector harmonic oscillators). In a QCD picture, this would correspond to the diagram of Fig. 11 where the dotted lines indicate the unitarity cut and the intermediate bare particles (quarks and gluons) are assumed to be ordered in rapidity. There we have isolated ladders of rapidity size y_1 and y_2, which clearly generate the corresponding Regge amplitudes. In the overlap region, two gluon ladders appear simutaneously and, from the t-channel point of view, a many-gluon state propagates. The relation between intermediate bare-particle states and the conven-

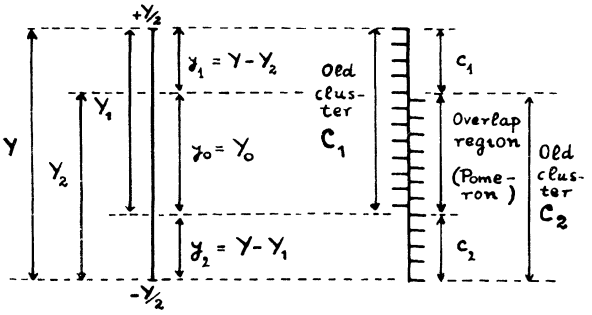

FIG. 10. Rearrangement of effective clusters in the rapidity plot.

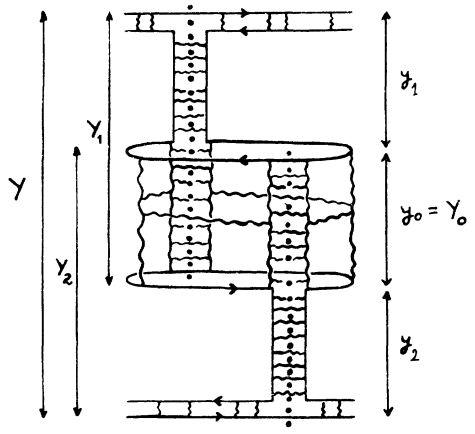

FIG. 11. Multiperipheral rearranging of effective clusters in terms of internal constituents. The dotted lines indicate the unitarity cut. Straight lines with arrows represent quarks and wavy lines stand for gluons.

tional n-particle intermediate states appears when we force each gluon to produce a $q\bar{q}$ pair. Then there is an obvious connection between the multiplicity and rapidity distribution of the gluons and the one of produced low-mass particles. We then expect each end c_1 and c_2 of the rapidity plot to contain only secondaries from clusters C_1 and C_2, respectively, with a multiplicity typical of that of planar amplitudes which build up the Regge trajectory α. In the overlap region both clusters contribute with nontrivial correlations dominated by nonleading exchanges. Experimentally the total multiplicity in production amplitudes grows roughly like $2.5 \ln s$, giving an average gap between light particles of about 0.4 units of rapidity which is small and opens the way to arguments based on daughter exchanges. Furthermore, when gaps are small, transverse momentum becomes important for the local dynamics so that we expect transverse dimensions to play an important role in the Pomeron sector.

In conclusion, we would like to emphasize that transverse components are crucial for the generation of the Pomeron although the kinematical picture is best understood in the rapidity variable, i.e., in a world with one effective space dimension. It is interesting to remark in this respect, that for a world with two dimensions no Pomeron appears in the string model[6] nor in QCD.[24] This can be understood since in this case there are no dynamical degrees of freedom left. In our phenomenological description in terms of quarks and gluons, this manifests itself through the fact that there is no triple-gluon coupling and therefore no "net" of gluons to fill in the overlap region.

VI. CONCLUSIONS

For the one-loop nonplanar orientable diagram, the analysis of the s-channel intermediate states leads to a consideration of two separate kinematical regions: $\gamma = s/s_1 s_2 \gg 1$ and $\gamma \ll 1$, $\gamma \sim 1$ corresponding to a transition region between both regimes. For $\gamma \gg 1$, we have the conventional multi-Regge dynamics which leads to the usual multiperipheral $f-\omega$ renormalization. For $\gamma \ll 1$, we have large values of $\tilde{t}$ longitudinal $\simeq -1/\gamma$ but no exponential cutoff is found. The accumulation of many resonances with all possible spins and of daughter exchanges seems to be what cancels the longitudinal-momentum cutoff at work in the peripheral amplitude, and the fact is that a powerlike behavior appears. The new Pomeron singularity dominates the sum rule for the rapidity overlap region and the remaining rapidity space is governed by the usual Regge amplitudes. In this way the Reggeon dipole appears to be coupled to a kernel which contains the Pomeron pole, as in the multiperipheral equation used by Pinsky and Snider.[9] The complete kernel is a sum of both multiperipheral and Pomeron contributions plus eventually some background term. As discussed in Sec. III, the dipole residue carries the required signature projectors which decouple the ω from the Pomeron and leave only a Pomeron daughter in the $C=-$ kernel. This would lead to the kind of phenomenological model presented in Sec. II, which as we have seen favors a weak f and ω renormalization, even in SU(2). But, of course, the underlying assumption is $\alpha_{P_0} > \alpha_f$, which depends on the details of the theory.[6,12]

The generalization of expression (28) to configurations with several massive clusters coming from the many-loop nonplanar orientable amplitude seems to be straightforward, although for technical reasons we have not been able to check it. This, together with the multi-Regge scheme for $\gamma \gg 1$, allows a reasonably complete classification of intermediate states with simple rules for computing their contribution to the imaginary part of the four-particle amplitude. We expect that the close connection which can be established between the dual-loop picture and the multiperipheral language will be helpful for the progress of the dual bootstrap.

Note. After completion of this work we received a paper by C. B. Chiu and S. Matsuda[25] dealing with analogous problems. In particular, they obtain a result similar to formula (28) for the production of two overlapping clusters.

ACKNOWLEDGMENTS

It is a pleasure to thank V. Alessandrini, X. Artru, J. Dash, R. Hong Tuan, K. Konishi, Alex Martin, and G. Veneziano for useful discussions. We are grateful to V. Alessandrini and A. Capella for a critical reading of the manuscript.

APPENDIX: NUMERICAL ILLUSTRATION OF THE SITUATION DESCRIBED IN SEC. II

We discuss here an almost trivial example in broken SU(3) where the cylinder has both a multiperipheral renormalization term and new signatured poles. We use standard one dimensional techniques. As in the original Chew-Rosenzweig model,[2] the cylinder is taken to be an SU(3) singlet, the breaking coming from the mass term in the Reggeon propagator [some SU(3) breaking could also be put in the cylinder via threshold factors, but it would only obscure the discussion at this stage]. As usual, we take a matrix formalism operating on the states $|1\rangle = (1/\sqrt{2})(u\bar{u} + d\bar{d})$ and $|2\rangle = s\bar{s}$. The Reggeon propagator is taken to be

$$R = \begin{pmatrix} \frac{1}{J-\alpha_1} & 0 \\ 0 & \frac{1}{J-\alpha_2} \end{pmatrix}, \tag{A1}$$

where α_1 (α_2) is the intercept of the planar trajectory built up from ordinary quarks (strange quarks).

The cylinder operator for the $C=+$ ($C=-$) channel is

$$K^{\pm} = \left(\pm k + \frac{\delta_{\pm}}{J-\alpha_{\pm}}\right)\begin{pmatrix} 2 & \sqrt{2} \\ \sqrt{2} & 2 \end{pmatrix}. \tag{A2}$$

The parameters k, δ_+, and δ_- should be positive in the physical region and they may depend on J. For simplicity we take them to be constants. As suggested by the analysis of Sec. III, the new negative-signatured pole is the daughter of the Pomeron so that $\alpha_- = \alpha_+ - 1$. We ignore the coupling of the Reggeons to the external particles, because they just act as overall normalization constants for each physical process. After iteration of $K^{\pm}R$ we get for the full amplitude

$$A^{\pm} = \frac{\pm k + \delta_{\pm}/(J-\alpha_{\pm})}{d^{\pm}(J)} \times \begin{pmatrix} \frac{2}{(J-\alpha_1)^2} & \frac{\sqrt{2}}{(J-\alpha_1)(J-\alpha_2)} \\ \frac{\sqrt{2}}{(J-\alpha_1)(J-\alpha_2)} & \frac{1}{(J-\alpha_2)^2} \end{pmatrix} + R, \tag{A3}$$

with

$$1 - d^{\pm}(J) = \frac{\delta_{\pm}}{J-\alpha_{\pm}}\left(\frac{2}{\alpha_{\pm}-\alpha_1} + \frac{1}{\alpha_{\pm}-\alpha_2}\right) + \frac{2}{J-\alpha_1}\left(\pm k - \frac{\delta_{\pm}}{\alpha_{\pm}-\alpha_1}\right) + \frac{1}{J-\alpha_2}\left(\pm k - \frac{\delta_{\pm}}{\alpha_{\pm}-\alpha_2}\right), \tag{A4}$$

and the residue matrix has to be evaluated at $d^{\pm}(J)=0$, which is the position of the new poles. For values of α_+ and α_- in the spirit of the Harari-Freund scheme, i.e., $\alpha_+ > \alpha_1 > \alpha_2 > \alpha_-$, the α_+ pole will always be renormalized upwards and the α_- pole moved downwards, which is very appealing phenomenologically. As for the trajectories α_1 and α_2, they can be displaced either way. In particular, a zero shift can be obtained for α_1 in both $C=+$ and $C=-$ channels if we require Eqs. (3a) and (3b) to be satisfied. This is different from the more conventional scheme where the residue of an unshifted trajectory vanishes and residues are proportional to shifts. The general solution can be written as

$$A^{+} = \sum_{j=1,+} \frac{g_j'^2}{J-\alpha_j'} \begin{bmatrix} \cos^2\theta_j & \sin\theta_j\cos\theta_j \\ \sin\theta_j\cos\theta_j & \sin^2\theta_j \end{bmatrix} + \frac{g_2^2}{J-\alpha_2'} \begin{bmatrix} \sin^2\theta_2 & \sin\theta_2\cos\theta_2 \\ \sin\theta_2\cos\theta_2 & \cos^2\theta_2 \end{bmatrix}, \tag{A5}$$

where the α''s are the new intercepts. A similar expression can be written for A^-.

With the conditions (3a) and (3b), and with the simple choice $\alpha_{P_0}=0.85$, $\alpha_1=0.5$, $\alpha_2=0.2$, and $k=0.05$ (which of course does not correspond to the best fit), we get

$$\delta_+ = 0.0175, \quad \delta_- = 0.0275$$

for $C=+$,

$$\begin{aligned} &\alpha_{\text{Pomeron}} = \alpha_+' = 0.98, \quad g_+^2 = 0.255, \quad \theta_+ = 23^\circ \\ &\alpha_1' = \alpha_f = 0.5, \quad g_f^2 = 0.78, \quad \theta_f = 0^\circ \\ &\alpha_2' = \alpha_{f'} = 0.22, \quad g_{f'}^2 = 0.84, \quad \theta_{f'} = -6^\circ \end{aligned} \tag{A6}$$

and for $C=-$,

$$\begin{aligned} &\alpha_-' = -0.33, \quad g_-^2 = 0.25, \quad \theta_- = 42^\circ \\ &\alpha_\omega = 0.5, \quad g_\omega^2\, 0.82, \quad \theta_\omega = 0^\circ \\ &\alpha_\phi = 0.23, \quad g_\phi^2 = 0.82, \quad \theta_\phi = -9^\circ. \end{aligned} \tag{A7}$$

Although the Pomeron has a weak coupling compared to the f, such a result in this kind of model is compatible with data up to ISR energies, as shown by Pinsky and Snider[9] provided that $\alpha_{\text{Pomeron}} > 1$, which is not difficult to obtain with a more accurate choice of parameters. If the present choice already produces the results (A6) and (A7), it is obvious that a realistic fit would not encounter serious problems, but this is not the goal of the present paper.

---

*Now at CERN, Geneva, Switzerland.

[1]G. Veneziano, Phys. Lett. 52B, 220 (1974); Nucl. Phys. B74, 365 (1974).

[2]H. M. Chan, J. E. Paton, and T. S. Tsun, Nucl. Phys. B86, 479 (1975); H. M. Chan, J. E. Paton, T. S. Tsun, and S. W. Ng, *ibid.* B92, 13 (1975); N. Papadopoulos, C. Schmid, C. Sorensen, and D. Webber, *ibid.* B101, 189 (1975); G. F. Chew and C. Rosenzweig, Phys. Lett. 58B, 93 (1975); Phys. Rev. D 12, 3907 (1975).

[3]H. Lee, Phys. Rev. Lett. 30, 719 (1973); G. F. Chew and C. Rosenzweig, Ref. 2.

[4]P. R. Stevens, G. F. Chew, and C. Rosenzweig, Nucl.

Phys. B110, 355 (1976).
[5]J. W. Dash, Phys. Lett. 61B, 199 (1976); J. W. Dash, S. T. Jones, and E. K. Manesis, Phys. Rev. D 18, 303 (1978).
[6]D. J. Gross, A. Neveu, J. Scherk, and J. H. Schwarz, Phys. Rev. D 2, 697 (1970). For a comprehensive review, see M. Jacob, *Dual Theory* (North-Holland/American Elsevier, Amsterdam, 1974).
[7]G.'t Hooft, Nucl. Phys. B75, 461 (1974); C. G. Callan, N. Coote and D. J. Gross, Phys. Rev. D 13, 1649 (1976); see also G. Veneziano, Ref. 8.
[8]G. Veneziano, Nucl. Phys. B108, 285 (1976); B117, 519 (1976).
[9]S. S. Pinsky and D. R. Snider, Phys. Rev. D 13, 1470 (1976); J. C. Romão and P. G. O. Freund, Nucl. Phys. B121, 413 (1977); D. B. Duke, Phys. Lett. 71B, 342 (1977).
[10]M. Ademollo, H. R. Rubinstein, G. Veneziano, and M. A. Virasoro, Phys. Rev. 176, 1904 (1968).
[11]V. Alessandrini, D. Amati and B. Morel, Nuovo Cimento 7A, 797 (1972).
[12]E. Cremmer and J. Scherk, Nucl. Phys. B50, 222 (1972).
[13]Y. Eylon, Nucl. Phys. B118, 119 (1977); M. Fukugita, T. Inami, N. Sakai, and S. Yazaki, *ibid.* B121, 93 (1977).
[14]H. M. Chan and T. S. Tsun, Nucl. Phys. B118, 413 (1977); B. R. Webber, Phys. Lett. 62B, 449 (1976).
[15]R. Hong Tuan, Orsay Report No. LPTHE 77/4 (unpublished).
[16]R. Hong Tuan, private communication and Orsay Report No. LPTHE 77/28 (unpublished).
[17]S. R. Amendolia *et al.*, Nuovo Cimento 31A, 17 (1976).
[18]M. I. Admovich *et al.*, Yad. Fiz. 22, 530 (1975) [Sov. J. Nucl. Phys. 22, 275 (1975)].
[19]M. T. Adamovich *et al.*, Nuovo Cimento 33A, 183 (1976).
[20]D. S. Chernavski, I. M. Dremin, T. I. Kanarek, and E. I. Volkov, P. N. Levedev Institute Report No. 40, 1976 (unpublished); M. I. Adamovich *et al.*, P. N. Levedev Institute Report No. 122, 1976 (unpublished).
[21]M. Anselmino, A. Ballestrero, and E. Predazzi, Nuovo Cimento 41A, 723 (1977); Ali H. Shehadeh and Euan J. Squires, J. Phys. G 3, L135 (1977).
[22]D. Amati, C. Bouchiat, and J. L. Gervais, Lett. Nuovo Cimento 2, 399 (1969).
[23]A. Neveu and J. Scherk, Nucl. Phys. B23, 630 (1970).
[24]R. C. Brower, J. Ellis, M. G. Schmidt, and J. M. Weis, Nucl. Phys. B128, 175 (1977); M. B. Einhorn and E. Rabinovici, *ibid.* B128, 421 (1977).
[25]C. B, Chiu and S. Matsuda, Nucl. Phys. B134, 463 (1978).

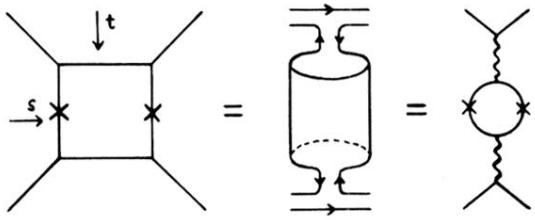

FIG. 1. The cylinder graph and topology.

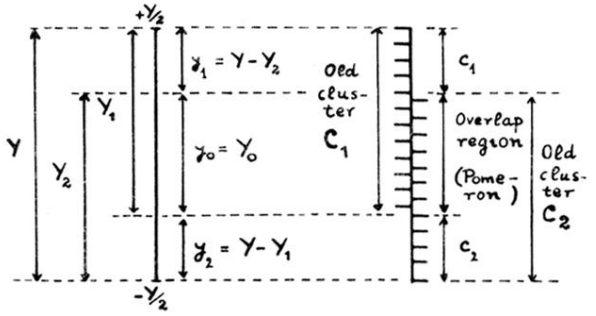

FIG. 10. Rearrangement of effective clusters in the rapidity plot.

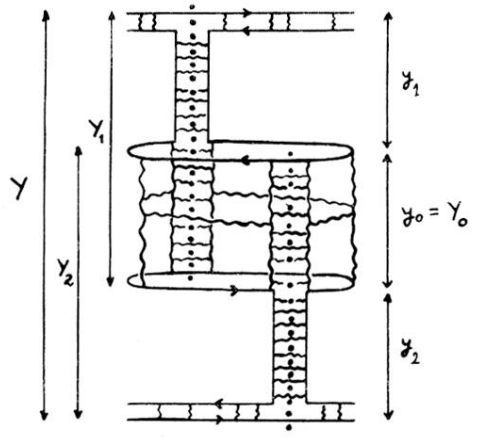

FIG. 11. Multiperipheral rearranging of effective clusters in terms of internal constituents. The dotted lines indicate the unitarity cut. Straight lines with arrows represent quarks and wavy lines stand for gluons.

(a) (b)

FIG. 2. (a) Propagation of leading-trajectory states. (b) Propagation of daughter-trajectory states or, in general, nonleading objects.

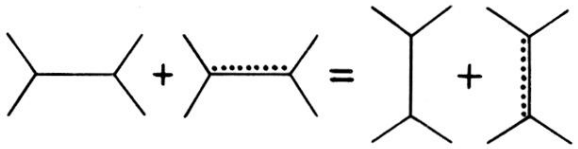

FIG. 3. Duality equation in terms of produced and exchanged leading and nonleading objects.

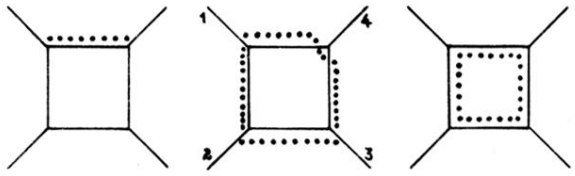

FIG. 4. Some graphs contributing to the whole one-loop planar diagram. (b) contains "radial excitations" propagating along internal lines between particle 1 and particle 2, between particle 2 and particle 3, and between particle 3 and particle 1.

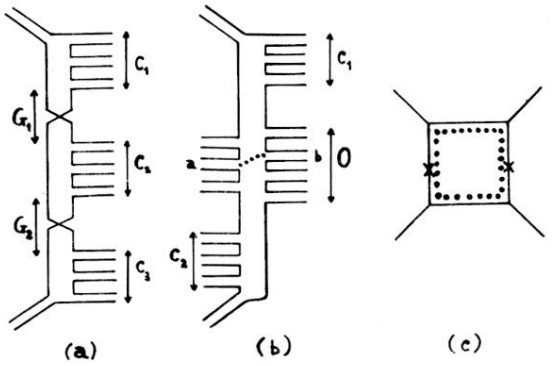

FIG. 5. (a) Conventional multiperipheral description of the n-particle intermediate states in terms of quark lines, clusters (C_i) and gaps (G_i). (b) An event which does not fit in the conventional scheme. O is the overlap region between particles emitted by both quark lines and the dotted line is a "radial excitation" traveling from particle a to particle b. (c) DFT description of the shadow of event (b).

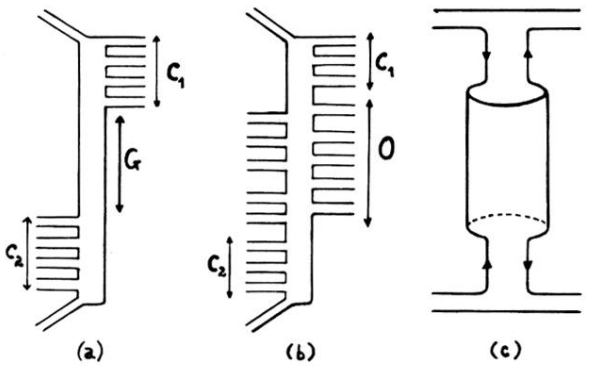

FIG. 6. (a) Multiperipheral contribution to the Pomeron dipole. (b) Nonmultiperipheral term carrying the same internal quantum numbers. (c) Topological and quark-line description of the shadow of both events (omitting holes).

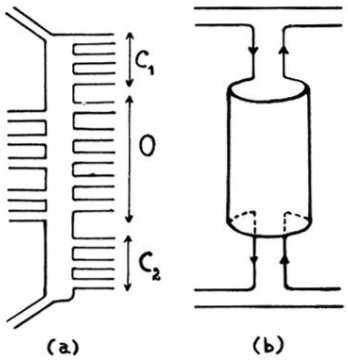

FIG. 7. (a) Another possible nonmultiperipheral contribution to the Pomeron dipole. (b) Topological and quark-line description of the shadow of this event (omitting holes).

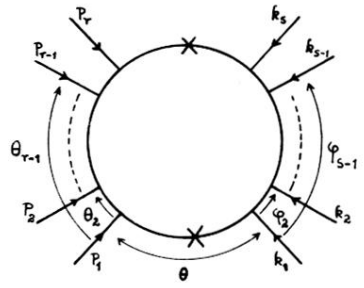

FIG. 8. N-particle one-loop cylinder diagram ($N = r + s$).

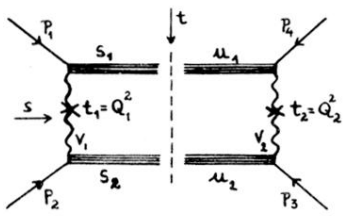

FIG. 9. Kinematics for the factorization in terms of two-massive-particle (or two-cluster) intermediate states. s_1 and s_2 are the squared masses of the intermediate objects, and Q_1 and Q_2 are the momenta of the exchanged twisted Reggeons. All external momenta are taken to be incident.